Fibronectin attenuates increased endothelial monolayer permeability after RGD peptide, anti-$\alpha_5\beta_1$, or TNF-α exposure

THERESA M. CURTIS, PAULA J. McKEOWN-LONGO, PETER A. VINCENT, SUZANNE M. HOMAN, ERIN M. WHEATLEY, AND THOMAS M. SABA
Department of Physiology and Cell Biology, Neil Hellman Medical Research Building, Albany Medical College, Albany, New York 12208

Curtis, Theresa M., Paula J. McKeown-Longo, Peter A. Vincent, Suzanne M. Homan, Erin M. Wheatley, and Thomas M. Saba. Fibronectin attenuates increased endothelial monolayer permeability after RGD peptide, anti-$\alpha_5\beta_1$, or TNF-α exposure. *Am. J. Physiol.* 269 (*Lung Cell. Mol. Physiol.* 13): L248–L260, 1995.—Endothelial permeability can be altered by tumor necrosis factor-α (TNF-α), a cytokine released in association with inflammation-induced tissue injury. In the subendothelial matrix, fibronectin (Fn) influences endothelial cell adhesion by the interaction of integrins with RGD and non-RGD attachment sites in Fn. We compared the effect of TNF-α, RGD-containing peptides (GRGDSP), or antibody to $\alpha_5\beta_1$-integrins on the protein permeability of bovine lung endothelial monolayers as assessed by transendothelial ^{125}I-labeled albumin clearance. We also examined the influence of purified human plasma fibronectin (hFn) on this permeability response. TNF-α, RGD peptides, and antibodies to $\alpha_5\beta_1$-integrins elicited a dose- and time-dependent increase in protein permeability as well as a reorganization and/or disruption of the endogenous Fn matrix. A control RGE peptide (GRGESP) as well as immunoglobulin G purified from nonimmune rabbit serum did not increase endothelial protein permeability or disrupt the endogenous fibrillar Fn pattern in the matrix. Likewise, a LDV peptide derived from the alternatively spliced type III connecting segment (IIICS) within bovine Fn (bFn) was unable to increase permeability of the bovine endothelial monolayer. Co-incubation of purified soluble hFn (300 or 600 μg/ml) with either TNF-α, the RGD peptide, or the antibody to $\alpha_5\beta_1$-integrins prevented the increase in endothelial permeability. This protective effect was also observed when the purified hFn (600 μg/ml) was added after the TNF-α-induced increase in endothelial permeability had taken place. Immunofluorescent analysis confirmed the incorporation of the hFn into the subendothelial matrix and its co-localization with the endogenous bFn. The similar alteration of the subendothelial matrix after exposure to RGD peptides, anti-$\alpha_5\beta_1$-antibodies, or TNF-α, coupled with the ability for hFn to attenuate the permeability increase typically elicited by all three agents, suggests that disruption of cell-matrix interactions may be the mechanism by which TNF-α alters endothelial permeability.

vascular permeability; integrins; lung permeability

FIBRONECTIN (Fn), an adhesive 440-kDa dimeric glycoprotein consisting of two very similar monomers held together by disulfide bonds (26), exists in a soluble form in plasma and lymph and in an insoluble form incorporated into the extracellular matrix (ECM). Plasma Fn can enhance the phagocytosis of gelatin-coated particles by macrophages as well as incorporate into various connective tissue and blood vessel matrices (4, 26). The tissue pool of insoluble Fn is believed to consist of a mixture of locally synthesized Fn as well as plasma-derived Fn (26). In the ECM, Fn can influence cell adhesion to a substratum. The cell binding activity of Fn in the matrix primarily resides in the Arg-Gly-Asp (RGD) sequence located within the III-10 module of Fn (21). This RGD sequence also exists in other adhesive proteins in the blood, such as vitronectin and fibrinogen. An alternatively spliced type III connecting segment domain in human Fn called IIICS, also known as the variable or V region, contains two non-RGD binding sites for cell-type specific adhesion. The two active sites for cell adhesion identified within IIICS of human Fn are the CS1 site (first 25 residues of IIICS) and the CS5 site (residues 90–109 of IIICS) (12). Endothelial cells have multiple integrin receptors on their surface that bind these various RGD and non-RGD "cell attachment" sites in matrix-localized Fn (17, 21). Such binding is believed to influence the integrity of the vascular barrier.

Endothelial permeability in the lung is increased during inflammation-induced septic lung injury (5, 26), an event associated with the release of cytokines such as tumor necrosis factor (TNF-α) from activated monocytes/macrophages (23, 32) in the lung microcirculation and interstitium. Increased lung endothelial permeability during postoperative or posttrauma sepsis is believed to be mediated by either pulmonary microembolization secondary to intravascular coagulation, endotoxin-induced cytokine secretion, or the release of proteases and/or oxygen metabolites from activated inflammatory cells sequestered in the lung (23, 26, 32). Such an increase in lung vascular permeability contributes to the pathogenesis of pulmonary edema and adult respiratory distress syndrome in septic surgical and trauma patients (26). TNF-α, a cytokine released from activated monocytes and macrophages, has been implicated as a mediator contributing to inflammation-induced lung vascular injury (23, 32). Recombinant TNF-α elicits cardiovascular and pulmonary disturbances similar to those observed during endotoxemia or septic shock (23). Moreover, infusion of antibodies to TNF-α reduces lethality to severe endotoxemia or bacteremia (32). Indeed, TNF-α decreases the integrity of the endothelial barrier as verified by both in vitro and in vivo studies (10, 23, 25, 36, 37).

The adherence of fibroblasts and endothelial cells to a Fn-containing substratum is disturbed by excess fluid phase small-molecular-weight peptides containing the RGD sequence (11, 21). However, the relationship of

1040-0605/95 $3.00

altered endothelial cell adhesion to both transendothelial protein permeability as well as subendothelial matrix integrity has not been investigated. We determined whether the effect of TNF-α on both lung endothelial protein permeability and organization of Fn in the subendothelial matrix could be reproduced by agents that disrupt cell-matrix interactions. To accomplish this goal, we compared the effect of TNF-α, RGD peptides, or antibody against $\alpha_5\beta_1$-integrin on both the protein permeability as well as the Fn-containing ECM of bovine lung endothelial cell monolayers. In addition, the effect of adding purified human fibronectin (hFn) to the culture medium on the endothelial permeability response after exposure to RGD peptides or anti-$\alpha_5\beta_1$-antibodies was compared with the protective effect observed after adding soluble hFn to TNF-α-treated monolayers.

METHODS

Endothelial Cell Monolayer

Calf pulmonary artery endothelial cells (CPAE; American Type Culture Collection CCL-209; Rockville, MD) were grown in Dulbecco's modified Eagle's medium (DMEM; GIBCO, Grand Island, NY) supplemented with 20% fetal bovine serum (FBS; Hyclone), nonessential amino acids (10 mm, GIBCO), penicillin (100 U/ml), and streptomycin (100 μg/ml). The cells were split 1:2 every fourth day. Experiments were performed between passages 19 to 23. For transendothelial protein clearance studies, the endothelial cells were seeded (75,000 cells/well) and grown to confluence (3–4 days) on tissue culture-treated Transwell filters (6.5 mm diam, 0.4 μm pore size, Nucleopore Polycarbonate Membrane; Costar, Cambridge, MA).

Because the Transwell filters are opaque, we were unable to view cells on filters by light microscopy. Accordingly, confluence was determined as previously documented (36, 37) by seeding endothelial cells on glass coverslips to which 6.5-mm chemotactic chambers had been glued. This allowed seeding densities (75,000) on the glass coverslips to be comparable to those on the filters. The endothelial monolayer on the glass coverslips was homogenous and cobblestone in appearance, as determined by phase-contrast microscopy (data not shown) by 3–4 days postseeding.

Protein Permeability Using the Dual Chamber Monolayer System

We used the dual-chamber monolayer technique to evaluate endothelial protein permeability (6, 36, 37). This technique allows for the measurement of transendothelial albumin flux in the absence of hydrostatic or oncotic pressure gradients (6). This in vitro model system consisted of a luminal chamber containing the tissue culture-ready filter, which was covered with a confluent monolayer of CPAE cells. A styrofoam collar around the luminal chamber allowed it to float in a larger abluminal chamber. This allowed us to maintain the fluid height in both chambers at the same level to eliminate a convective flux across the monolayers. The fluid in the abluminal chamber was stirred constantly during the experiment. Both chambers were kept at 37°C using a thermostatically controlled water bath. Previous studies (28) have shown that this CPAE monolayer model selectively restricts molecules according to their size, which is very similar to the in vivo restrictive behavior of the lung vascular barrier to proteins.

Measurement of ^{125}I-labeled albumin clearance (μl/min) as described by Cooper et al. (6) was used to quantify the changes in the diffusive permeability of albumin across the endothelial monolayers. In this procedure, we added 25 ml of low glucose DMEM supplemented with 0.5% bovine serum albumin (BSA) to the abluminal chamber. We removed the medium from the luminal chamber after exposure of the endothelial monolayer to either TNF-α, synthetic peptides, or antibody to $\alpha_5\beta_1$-integrins, and then added 200 μl of the same BSA-containing DMEM solution that was in the abluminal chamber, as well as the ^{125}I-albumin tracer. To measure albumin clearance, we collected 400-μl aliquots of the medium from the abluminal chamber every 5 min over a 60-min interval and assayed for ^{125}I radioactivity using a TM Analytic 1193 gamma counter.

Calculation of Endothelial Albumin Permeability

As previously described (6, 36, 37), the volume of the luminal chamber that is cleared of the ^{125}I-albumin tracer as it enters into the abluminal chamber represents the total activity of the abluminal chamber. The change in clearance volume during each 5-min interval between sampling points was calculated by dividing the amount of albumin flux during the interval by the tracer concentration in the luminal chamber. The clearance volume of albumin at each time point (V_{Alb_t}) was calculated by summing the incremental clearance volumes as described by the equation

$$V_{Alb_t} = \sum_{i=1}^{t} \frac{V_{A_i} \times \Delta[A]_i}{[L]_i}$$

where V_{Ai} is the volume in the abluminal chamber at each time point, $\Delta[A]_i$ is the increase in tracer concentration between time points, and $[L]_i$ is the tracer concentration in the luminal chamber at each time point. This approach accounts for changes in the chamber volumes due to sampling, since the chamber volumes were constant between sampling points. The change in V_{Alb} over time (dV_{Alb}/dt), which is equal to the clearance expressed in units of microliters per minute, was determined as previously described (6, 36, 37) by weighted least-squares nonlinear regression for all 5-min experimental time intervals over the 5- to 60-min test period.

Radiolabeled Albumin

Bovine albumin (Sigma, St. Louis, MO) was iodinated with Na^{125}I, using the chloramine-T method as previously described (36, 37). Five millicuries of ^{125}I were combined with 100 mg of albumin. The ^{125}I-albumin was maintained in dialysis against phosphate-buffered saline (PBS, pH 7.4) until used. The ratio of free to protein-bound ^{125}I was determined by using centricon 30 microconcentrator filters (Amicon), and we only used preparations that had $< 0.5\%$ free ^{125}I.

Human Plasma Fn Preparation

We used purified human plasma Fn (hFn) that was prepared and provided to our laboratory in a pasteurized and lyophilized form (RHCG; USV/Armour Pharmaceuticals). This hFn has been previously used for both in vitro as well as in vivo studies, including a phase II clinical study in septic and non-septic surgical patients (26, 27). It enhances the phagocytosis of gelatin-coated particles by macrophages (26, 27) and retains its ability to be rapidly incorporated into the ECM of the lung and other tissues after intravenous injection (4) as well as into the subendothelial matrix of substrate-attached lung endothelial cells in culture (36).

Antibodies

Protein A-purified rabbit polyclonal antibodies to human $\alpha_5\beta_1$-integrin receptors were commercially obtained (GIBCO

BRL). This antibody has no cross-reactivity with the human vitronectin receptor ($\alpha_v\beta_3/\beta_5$), hFn, or other human plasma proteins, as verified by Western blot analysis. Because this is a polyclonal antibody, it contains a collection of antibodies to both the α_5- and β_1-integrin subunits, thus rendering it capable of cross-reacting with all β_1-containing integrins. Immunoglobulin (Ig) G purified from normal nonimmune rabbit serum using protein A (Pharmacia; San Diego, CA) was used as a control. Both IgG preparations were dialyzed against DMEM before use in the experiments. For the immunofluorescent studies, we used rabbit antiserum to bovine fibronectin (bFn) (Calbiochem, La Jolla, CA), followed by rhodamine-isothiocyanate (RITC)-conjugated goat anti-rabbit IgG (Cappel Organon Teknika, Durham, NC) and fluorescein isothiocyanate (FITC)-conjugated goat anti-human Fn (Cappel Organon Teknika). To assure specificity of the antibodies and avoid cross-reactivity, the antibodies to either bFn or hFn were subjected to affinity chromatography against the opposite species antigen using either hFn or bFn Sepharose columns, respectively.

Experimental Protocols

TNF-α. The endothelial monolayers were incubated with purified recombinant human TNF-α (Cellular Products, Buffalo, NY), which had specific activity of 24×10^6 units/mg protein. To determine the optimal dose of TNF-α required to elicit a consistent increase in protein permeability, the monolayers were first exposed to purified TNF-α at concentrations of either 100, 200, or 400 units/ml of culture medium (DMEM containing 5% FBS) for 18 h. Based on the dose-response experiment, endothelial monolayers were then exposed to TNF-α at a fixed concentration of 200 units/ml for either 0, 6, or 18 h to determine the time course for the alteration of protein permeability. The endothelial monolayers were then treated with TNF-α (200 units/ml) for 18 h in conjunction with various concentrations of hFn (5, 10, 25, 50, 100, 300, 600 μg/ml) in the medium. Confluent monolayers not exposed to TNF-α were also treated with either 50, 100, 200, 300, or 600 μg/ml of hFn alone in the medium for 18 h. Experiments were also performed to determine if soluble hFn could actually reverse the TNF-α-induced increase in permeability, after the endothelial monolayers were exposed to purified TNF-α for 18 h at a concentration of 200 units/ml, since this incubation time and dose caused a maximal increase in protein permeability. In this set of experiments, the TNF-α-containing medium was removed after 18 h, and fresh medium with or without purified hFn (600 μg/ml) was added for an additional 6 h before measuring protein clearance. It should be noted that the current in vitro protection experiments were an extension of our previous in vivo studies in sheep on the protective effect of hFn intravenous therapy on lung protein permeability and the relationship of plasma Fn levels to lung vascular permeability (4, 5, 26, 27). In sheep, the normal plasma Fn concentration is usually 575–625 μg/ml (5), thus 600 μg hFn/ml culture medium was selected as our optimal test dose in the current in vitro studies. For reference, normal human Fn levels are ~300–400 μg/ml (27).

Synthetic peptides. Endothelial monolayers were incubated for 18 h with the RGD-containing GRGDSP peptide (GIBCO BRL) or the control GRGESP peptide (GIBCO BRL) at a concentration of either 0.50 or 1.0 mg peptide/ml culture medium (DMEM containing 0.2% BSA). To determine the importance of non-RGD cell binding sites in Fn on the permeability of the bovine endothelial monolayer, the cell layers were also incubated with the tripeptide LDV, which corresponds to the active adhesion/attachment site contained in the CS1 region within the IIICS domain of bFn. The tetrapeptide, REDV, a second non-RGD attachment site found in the CS5 region of the IIICS domain of hFn, is not present in bFn. Thus an REDV-containing peptide was not used in the current study.

Anti-$\alpha_5\beta_1$. Endothelial monolayers were first incubated for varying intervals with antibodies against $\alpha_5\beta_1$-integrins at a concentration of 100 μg/ml of culture medium (DMEM containing 0.2% BSA) to identify the incubation interval that gave the optimal increase in permeability. In selected experiments, hFn (600 μg/ml) was added in conjunction with the antibody (100 μg/ml) for 24 h.

Dual-Label Immunofluorescence, Indirect Immunofluorescence, and Differential Interference Contrast Microscopy

CPAE cells were seeded (280,000 cells/well) on glass coverslips in 12-well tissue culture dishes and grown to confluence (3–4 days). Dual-label immunofluorescence was used to allow simultaneous detection of endogenous bFn and exogenously added hFn. The Fn matrix was examined after the CPAE monolayers were exposed to either the TNF-α, RGD peptide, RGE peptide, rabbit polyclonal antibody to $\alpha_5\beta_1$-integrins, or the IgG purified from nonimmune rabbit serum. These agents were added to the confluent monolayers in the presence or absence of 600 μg/ml hFn.

To examine both the bFn and hFn in the matrix of the bovine lung endothelial monolayers, the cells were rinsed three times with PBS (pH 7.4) and fixed in 3.0% formaldehyde in PBS for 15 min. After fixation, endothelial cell monolayers were rinsed three times with PBS and the monolayers were permeabilized with a *N*-2-hydroxyethylpiperazine-*N*′-2-ethanesulfonic acid (HEPES) solution containing 0.5% Triton X-100 on ice for 5 min, followed by three rinses with PBS. The cell monolayers were then blocked with 2% BSA + 50 mM glycine + 0.2% Tween 20 in PBS for 1 h. bFn in the matrix was stained for 1 h using species-specific rabbit antiserum to bFn (1:100 in PBS). At the same time in the dark, the exogenously added hFn was detected using FITC-conjugated goat anti-hFn (1:50 in PBS), which did not cross-react with the bFn. The cells were washed three times (10 min) with PBS and then incubated for 1 h with RITC-conjugated goat anti-rabbit IgG (1:50 in PBS). Control studies using no primary antibody were negative. The coverslips were again washed three times (10 min) in PBS and mounted in glycerol gelatin.

The slides were kept in the dark until they were viewed and photographed at a magnification of ×40 with Tmax film (Eastman Kodak), using a fluorescent microscope (Nikon microphot SA). The CPAE monolayers were also viewed using differential interference contrast (DIC) microscopy and photographed using Tmax film at a magnification of ×40 (Nikon microphot SA). When the endothelial cell layers were stained for only endogenous bFn after incubation with either TNF-α, RGD peptide, or antibodies to $\alpha_5\beta_1$-integrins, we utilized indirect immunofluorescence. For this approach, all procedures were identical to those described above for dual-label immunofluorescence, except that the FITC-conjugated antibody to the hFn was not added to the cells on the coverslips.

DNA Determination

CPAE cells were seeded (280,000 cells/well) in 12-well tissue culture dishes and grown to confluence (3–4 days). DNA content was analyzed according to the method of Rago et al. (22) with minor modifications. Briefly, cells were washed three times with PBS (pH 7.4) and then 0.5 ml of distilled water was added to each well and the plates were frozen at −20°C. Samples were thawed and 0.5 ml of TNE buffer (10 mM

tris(hydroxymethyl)aminomethane base, 1 mM EDTA, 2 M NaCl, pH 7.4) was added and mixed thoroughly. A 100-μl sample was added to 1,900 μl of the TNE solution containing bisbenzamide (2 μg/ml, Sigma). Fluorescence was measured using a fluorometer at an excitation of 365 nm and an emission of 460 nm. Calf thymus DNA (Sigma) was used for standards. Values are presented as micrograms DNA per well ± SE. Each value represents the average of 4–5 wells.

Statistical Methods

All experiments were performed at least in duplicate. Data are presented as means ± SE. Data were analyzed by one-way analysis of variance with significance from controls determined by a Newman-Keuls test. A confidence level of 95% ($P < 0.05$) was used to establish statistical significance.

RESULTS

We first determined if confluent lung endothelial monolayers seeded onto tissue culture-ready filters would display an increment in protein permeability after TNF-α, similar to the response we observed with TNF-α, using endothelial cells seeded onto gelatin-coated polycarbonate filters (36, 37). Presented in Fig. 1 is the protein permeability across the lung endothelial monolayers on tissue culture-ready filters, as influenced by having TNF-α in the culture medium for 18 h at a concentration of either 100, 200, or 400 units/ml. As shown in Fig. 1, protein clearance across the normal confluent lung endothelial monolayer was ~0.03 μl/min. TNF-α resulted in a significant ($P < 0.05$) increment in protein clearance, with a maximal response observed at 200 units of TNF-α/ml medium. Thus, although gelatin coating of polycarbonate filters may facilitate the initial attachment of endothelial cells (36, 37), once grown to confluence on either gelatin-coated polycarbonate filters or tissue culture-ready filters, the lung endothelial monolayers display a very similar increase in protein permeability after TNF-α exposure. Using TNF-α at a concentration of 200 units/ml, we then observed that TNF-α caused a significant ($P <$ 0.05) increase in endothelial permeability equivalent to at least 100% above baseline, even by 6 h (Fig. 2).

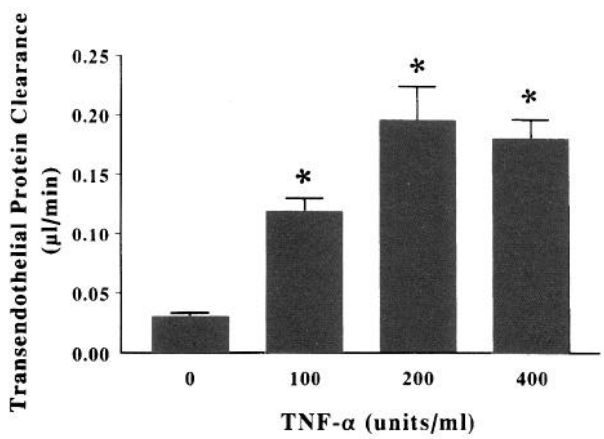

Fig. 1. The effect of human recombinant tumor necrosis factor-α (TNF-α) on protein permeability of calf pulmonary artery endothelial monolayers seeded onto tissue culture-ready wells. Once the cells reached confluence, the monolayers were incubated for 18 h with TNF-α at a dose of either 100, 200, or 400 units/ml. Values for protein clearance (μl/min) represent the means ± SE with 9–12 wells/group. *Significantly ($P < 0.05$) different from control without TNF-α.

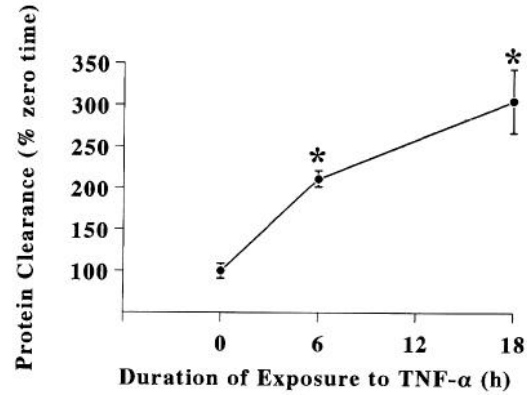

Fig. 2. Temporal effect of human recombinant TNF-α on protein permeability of calf pulmonary artery endothelial monolayers. Once the cells reached confluence, the monolayers were incubated for 0, 6, or 18 h with TNF-α at a dose of 200 units/ml. Values for protein clearance (% zero time) represent the means ± SE with 7–16 wells/group. Levels are expressed as a % of zero time baseline. *Significantly ($P < 0.05$) different from control without TNF-α.

Based on the time- and dose-response findings (Figs. 1 and 2), we used 200 units/ml of TNF-α and employed an 18-h incubation interval in the protection experiments with hFn. First, we co-incubated the TNF-α (200 units/ml) and the purified hFn with the confluent endothelial monolayers for 18 h. As shown in Fig. 3, hFn concentrations of either 300 or 600 μg/ml significantly ($P < 0.05$) attenuated the TNF-α-induced increase in protein permeability. Next, we added hFn to the medium after exposure of the endothelial cells to TNF-α to determine if hFn would also reverse an increase in permeability already induced by TNF-α. To do this study, TNF-α (200 units/ml) was first incubated with the cells for 18 h and then the TNF-α-containing medium was removed. New culture medium containing either 600 μg/ml hFn or no hFn was then added to the endothelial cell monolayers

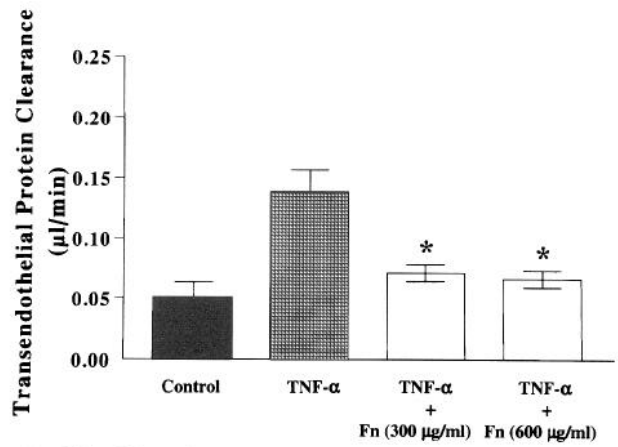

Fig. 3. The ability for soluble human plasma fibronectin (hFn) to attenuate the TNF-α-induced increase in lung endothelial permeability. Once the cells reached confluence, the monolayers were incubated for 18 h with TNF-α (200 units/ml) either alone or in parallel with the purified human plasma Fn at two concentrations. Control wells were supplemented with medium alone for 18 h. Values for protein clearance (μl/min) represent the means ± SE with 4 wells/group. *Significantly ($P < 0.05$) lower than TNF-α in the absence of hFn.

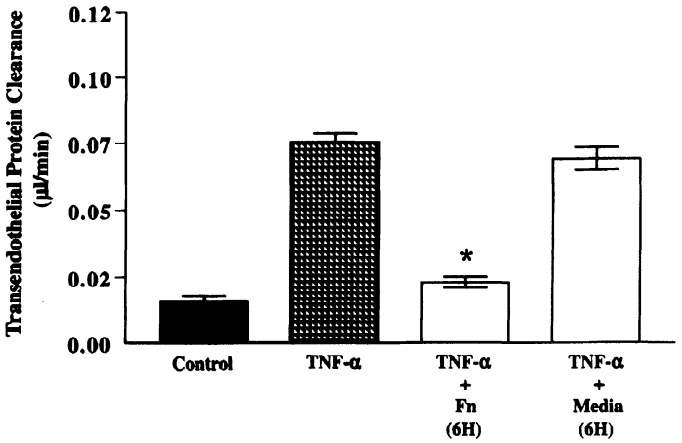

Fig. 4. Effect of adding soluble human plasma Fn to monolayers already preexposed to TNF-α. Confluent endothelial monolayers were treated with TNF-α (200 units/ml) for 18 h and then the treatment was either not removed, removed and replaced with medium containing 600 μg/ml hFn, or removed and replaced with medium alone for 6 h. Control wells were medium alone for 24 h. Values represent the means ± SE with 3–7 wells/group. *Significant ($P < 0.05$) protection was seen with Fn incubation for 6 h.

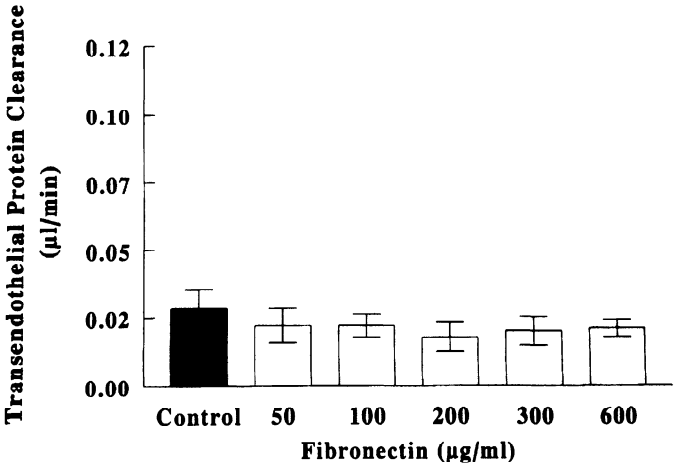

Fig. 6. The effect of soluble hFn on endothelial protein permeability. Once the cells were confluent, the monolayers were incubated with various concentrations of hFn for 18 h. Control wells received medium alone for 18 h. Values for protein clearance (μl/min) represent the means ± SE with 5–7 wells/group.

for an additional 6 h. With TNF-α alone for 24 h, we observed an increase in protein clearance that was four to five times over control baseline values (Fig. 4). As shown in Fig. 4, after the 18-h incubation with TNF-α, the subsequent addition of fresh medium without hFn for 6 h did not reverse the increase in permeability, but the addition of hFn containing fresh culture medium for the last 6 h rapidly reversed the abnormal protein clearance back to control values. Actually, the magnitude of the protection when the hFn was added in parallel with the TNF-α or when the hFn was added after the TNF-α-induced increase in permeability had already taken place was very similar.

We then determined the minimum amount of hFn needed to attenuate the increase in permeability caused by TNF-α. Figure 5 shows endothelial monolayers coincubated with TNF-α and varying concentrations of hFn for 18 h. hFn at concentrations of 600 and 300 μg/ml was able to completely attenuate the increase in permeability. At concentrations of hFn ranging between 25 and 100 μg/ml, protein clearance could be significantly ($P < 0.05$) reduced but not totally normalized to control levels. At an hFn concentration of 10 μg/ml, we observed a limited but statistically significant ($P < 0.05$) protection. When hFn was added at 5 μg/ml, the protective effect was lost. It is of interest that the dissociation constant (K_d) for the Fn matrix assembly site is 3.9×10^{-8} M (18), which means that soluble Fn in the culture medium at a concentration of 10–20 μg/ml should saturate 50% of all available Fn matrix assembly sites. The fact that there is partial protection with hFn at a level 10 μg/ml is consistent with these K_d values. To determine if there is an individual effect of soluble hFn on the protein clearance of normal endothelial layers in the absence of TNF-α exposure, varying concentrations of hFn alone were also added for 18 h to normal confluent endothelial monolayers (Fig. 6). No significant

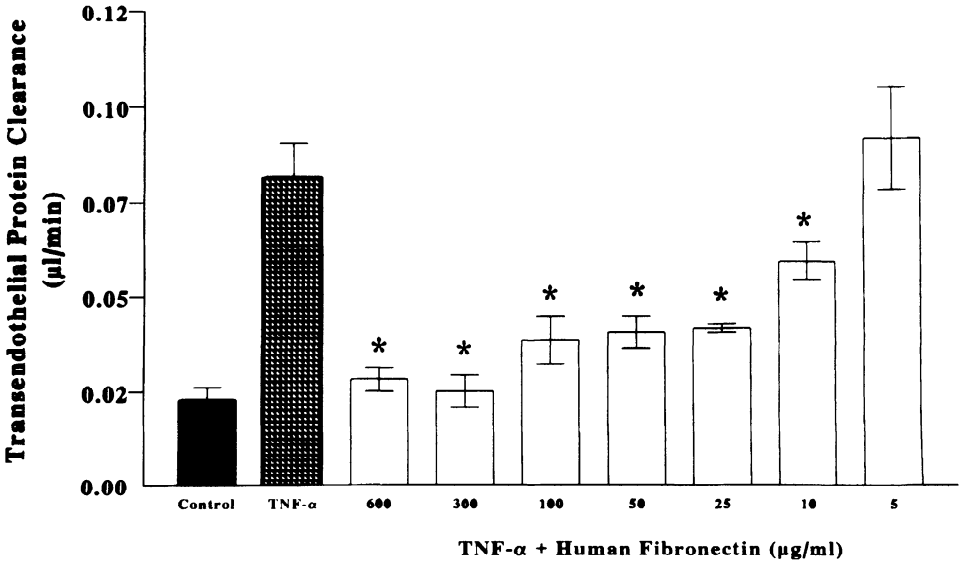

Fig. 5. The minimum concentration of hFn needed to attenuate the increase in permeability caused by TNF-α. Once the cells reached confluence, the monolayers were incubated for 18 h with TNF-α (200 units/ml) either alone or in conjunction with purified hFn at concentrations of 5–600 μg/ml medium. Control wells represented cells exposed to treatment medium alone for 18 h. Values for protein clearance (μl/min) represent the means ± SE with 3–12 wells/group. *Significantly ($P < 0.05$) lower than TNF-α without hFn.

($P > 0.05$) change from control baseline clearance values was seen with hFn concentrations even up to 600 μg/ml.

Endothelial monolayer integrity on a Fn-containing substratum is believed to be influenced by the interaction of the cell surface integrins with both RGD and non-RGD attachment sequences in matrix-localized Fn. Because we speculated that TNF-α may be exerting its effects by indirectly causing a change in cell-substrate interaction, we compared the effect of soluble synthetic peptides corresponding to both the RGD and non-RGD sites in bFn on protein permeability. Accordingly, we compared the permeability response of the monolayer to both an RGD-containing six-amino acid peptide (GRGDSP) and a control RGE-containing six-amino acid peptide (GRGESP). A three-amino acid peptide (LDV) from the CS1 domain within the IIICS region of Fn was also examined, since it represents the non-RGD cell attachment site in bFn. Incubation of the GRGDSP peptide with the monolayer for 18 h but not the GRGESP or LDV peptides resulted in a dose-dependent increase ($P < 0.05$) in protein permeability (Fig. 7). Purified hFn added to the medium at a concentration of either 300 or 600 μg/ml completely attenuated ($P < 0.05$) the RGD peptide effect on endothelial permeability (Fig. 8).

To define the importance of the interaction of $\alpha_5\beta_1$-integrin receptors with the RGD sequence in matrix-localized fibronectin on endothelial protein permeability, we then evaluated the effect of the antibodies to cell surface $\alpha_5\beta_1$-integrins on monolayer permeability. As shown in Fig. 9, antibodies against $\alpha_5\beta_1$-integrins (100 μg/ml) caused a time-dependent increment in endothelial protein permeability. Specificity was apparent, since IgG purified from nonimmune rabbit serum by protein A, which we used as a control, did not increase monolayer permeability (Fig. 10). Moreover, the increase in endothelial permeability in the presence of antibodies to $\alpha_5\beta_1$-integrins (100 μg/ml) was completely attenuated ($P < 0.05$) if the culture medium was supplemented with purified soluble hFn at a concentration of 600 μg/ml medium (Fig. 10).

To determine if the increase in protein permeability of the lung bovine endothelial monolayers was associated with a disruption and/or reorganization of endogenous bFn in the subendothelial matrix, we then utilized immunofluorescence to examine the Fn in the matrix of treated monolayers. Disruption of the endogenous bFn matrix was not seen after incubation of the endothelial cell layer with either the control RGE peptide or the control IgG molecule purified from nonimmune rabbit serum (immunofluorescence not shown). In contrast, as

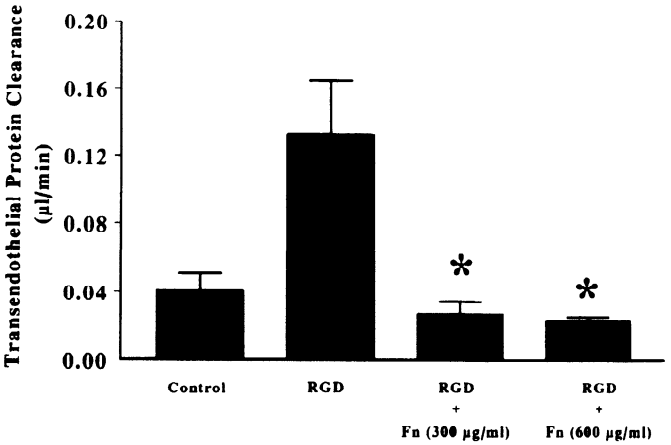

Fig. 8. The ability for soluble human plasma Fn to attenuate the RGD-induced increase in lung endothelial protein permeability. Confluent endothelial monolayers were incubated for 18 h with RGD peptides (0.5 mg/ml) either alone or in combination with human plasma fibronectin (300 or 600 μg/ml). Control wells received medium over the 18-h period. Values represent the means ± SE with 4 wells/group. *Significantly ($P < 0.05$) lower than protein clearance with the RGD peptide in absence of hFn.

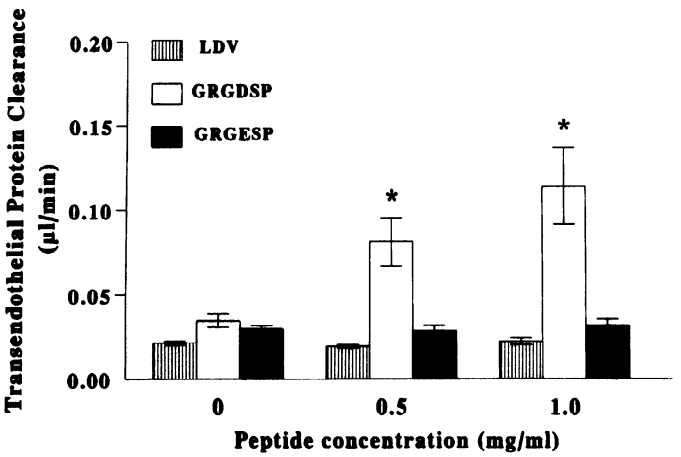

Fig. 7. Comparative effect of synthetic peptides on lung endothelial protein permeability. Confluent monolayers were incubated for 18 h with the peptide LDV derived from the connecting segment (CS)1 site in the IIICS domain of bovine Fn. RGD-containing peptides (GRGDSP) and RGE-containing peptides (GRGESP) were also added to confluent endothelial monolayers for 18 h. All peptides were added at concentrations of 0.5 and 1.0 mg/ml. Values represent the means ± SE with 4–9 wells/group. *Significantly ($P < 0.05$) different from control without the GRGDSP peptide.

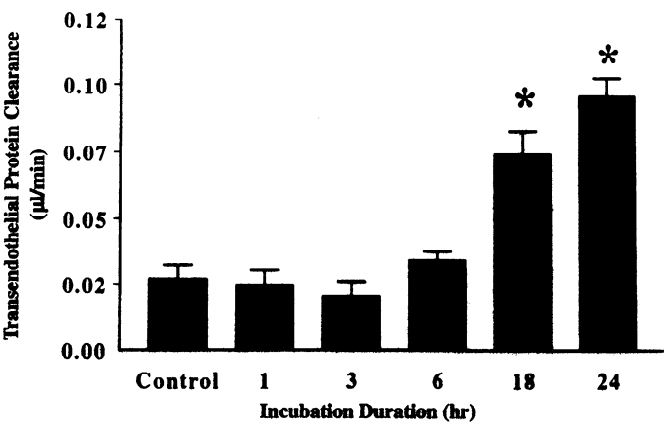

Fig. 9. Effect of polyclonal antibodies against the $\alpha_5\beta_1$-Fn integrin on protein permeability of lung endothelial monolayers. Confluent monolayers were supplemented with 100 μg/ml of protein A-purified immunoglobulin G (IgG) directed against the $\alpha_5\beta_1$-Fn integrin and incubated at 37°C for intervals of 1–24 h. Values represent the means ± SE with 4 wells/group. Control wells received no antibody, and clearance was assayed after 24 h. *Significantly ($P < 0.05$) different than control with no antibody.

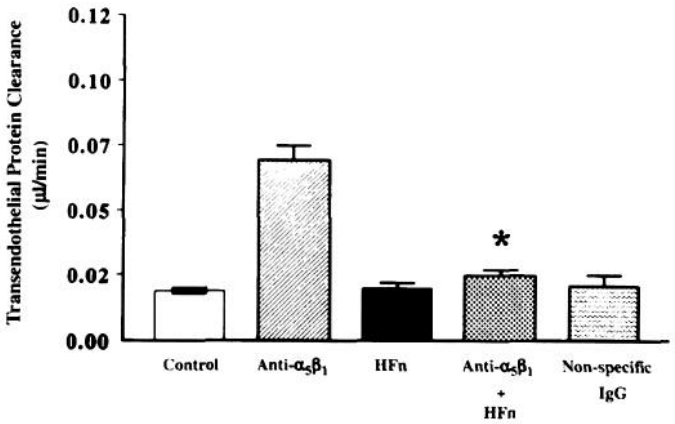

Fig. 10. The ability for purified human plasma Fn to attenuate the anti-$\alpha_5\beta_1$-induced increase in endothelial protein permeability. Confluent endothelial monolayers were incubated for 24 h with IgG directed against the $\alpha_5\beta_1$-Fn integrin (100 μg/ml) either alone or in combination with human plasma Fn (600 μg/ml). Specificity of the response was demonstrated by the lack of an increase in permeability by monolayers incubated with IgG from nonimmune rabbit serum (100 μg/ml) for 24 h. Wells were also treated with hFn alone for 24 h. Control wells were subjected to only the treatment medium for 24 h. Values represent the means ± SE with 4–12 wells/group. *Significantly ($P < 0.05$) lower than protein clearance with anti-$\alpha_5\beta_1$ in the absence of hFn.

shown in Fig. 11, after incubation of the monolayer with RGD peptides (Fig. 11*C*) or polyclonal antibody to the $\alpha_5\beta_1$-integrins (Fig. 11*D*), we observed a disrupted or reorganized endogenous bFn matrix that was very similar to that observed after treatment of the endothelial monolayer with purified TNF-α (Fig. 11*B*). All three treatments clearly altered the fibrillar Fn-rich matrix observed in normal endothelial cell layers examined at the same time (Fig. 11*A*).

When the culture medium was supplemented with purified hFn (600 μg/ml), incorporation of the hFn into the subendothelial matrix as well as its co-localization with the endogenous bFn was clearly apparent by immunofluorescence, using antibodies specific to hFn. This response was observed when hFn was added to monolayers treated with either TNF-α (Fig. 12), RGD peptides (Fig. 13), or antibodies to $\alpha_5\beta_1$-integrins (Fig. 14). When the CPAE cells were examined using DIC microscopy after treatment with TNF-α, RGD peptides, or anti-$\alpha_5\beta_1$-integrins, the presence of gaps or holes between endothelial cells in the monolayer was readily observed (arrows in Fig. 15, *B*, *C*, and *D*) in comparison to normal (Fig. 15*A*). When these same permeability increasing agents were added to the culture medium in the presence of purified hFn (600 μg/ml), the gaps

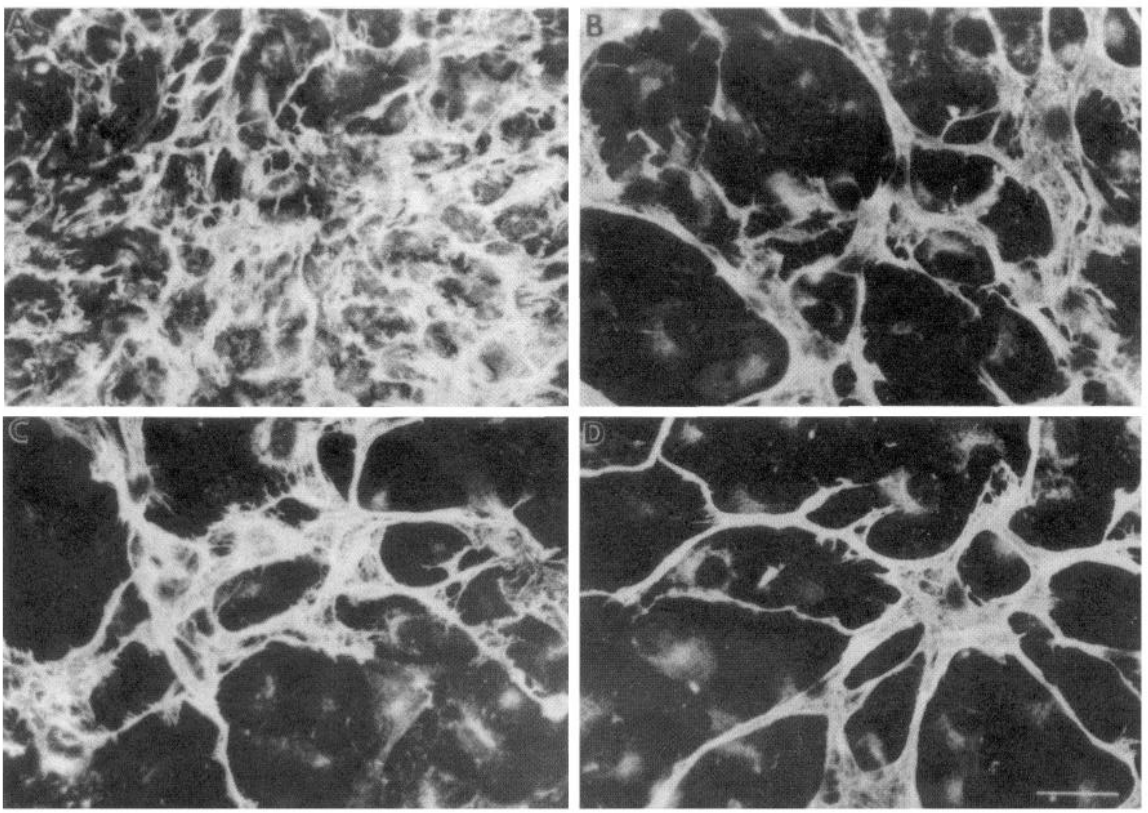

Fig. 11. Immunofluorescent examination of endogenous bFn in calf pulmonary artery endothelial (CPAE) monolayers after treatment with TNF, RGD, or anti-$\alpha_5\beta_1$-integrins. Confluent monolayers (3–4 days postseeding) were incubated for 18 h with either TNF-α (200 units/ml) or RGD (0.5 mg/ml). Monolayers were also incubated for 24 h with anti-$\alpha_5\beta_1$-integrin (100 μg/ml) before the assay. Control monolayers were exposed to medium alone for 24 h. Cells were permeabilized and the bovine Fn matrix was stained using rabbit antiserum to bovine Fn and rhodamine isothiocyanate (RITC)-conjugated goat anti-rabbit IgG. *A*: Fn-rich matrix of normal monolayers. *B*: TNF-α treated monolayers. *C*: RGD-treated monolayers. *D*: anti-$\alpha_5\beta_1$-integrin-treated monolayers. Bar = 40 μm.

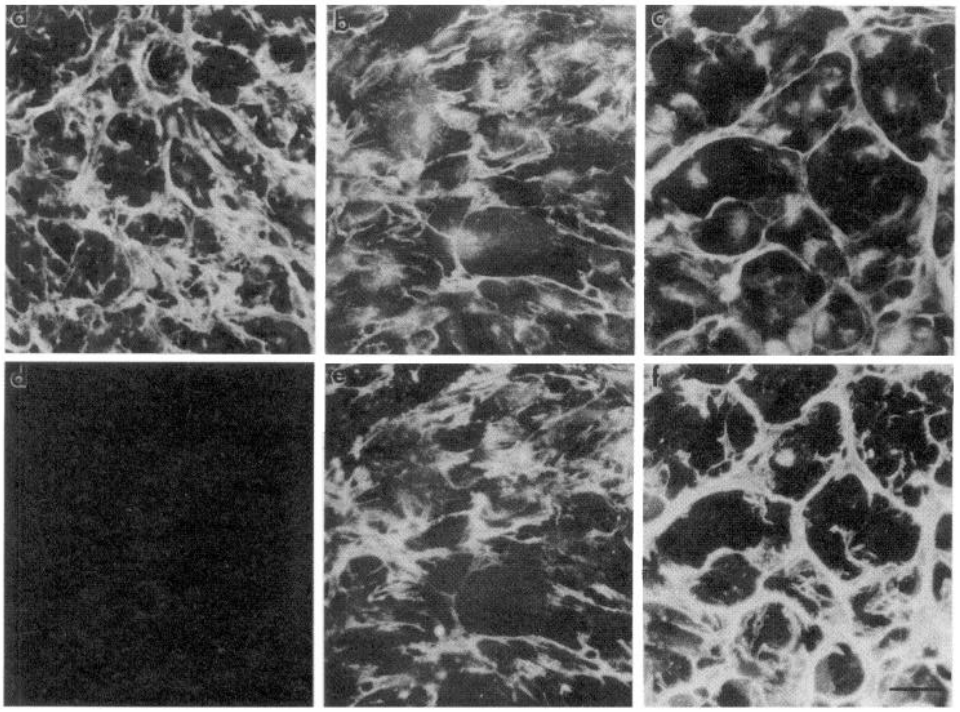

Fig. 12. Localization of exogenously added hFn in the matrix of CPAE monolayers co-incubated with both TNF-α and hFn. RITC fluorescence specific for bovine fibronectin antigen (*top*) and fluorescein isothiocyanate (FITC) fluorescence specific for human fibronectin antigen (*bottom*) are shown. *A-C*: RITC fluorescence of CPAE monolayers fixed and permeabilized at 0, 6, and 18 h, respectively after treatment of cells with TNF-α (200 units/ml) + hFn (600 μg/ml). *D-F*: FITC fluorescence of the identical monolayers at 0, 6, and 18 h, respectively. Bar = 40 μm.

between the cells essentially disappeared and the cell layer displayed a more flattened and cobblestone appearance (Fig. 15, *F*, *G*, and *H*) analogous to that observed in normal endothelial monolayers (Fig. 15*E*).

Exposure of the endothelial monolayers to TNF-α, RGD peptides, and the antibody to $\alpha_5\beta_1$-integrins, at the times and doses used in the current study, did not cause appreciable cell detachment. DNA content for monolayers treated with TNF-α (200 units/ml) for 18 h was 1.23 ± 0.07 vs. 1.30 ± 0.03 μg DNA/well ($P > 0.05$) for controls exposed to only medium. Monolayers were also treated with RGD peptides (0.5 mg/ml) for 18 h or an antibody to $\alpha_5\beta_1$-integrins (100 μg/ml) for 24 h before DNA content was examined. Control monolayers ex-

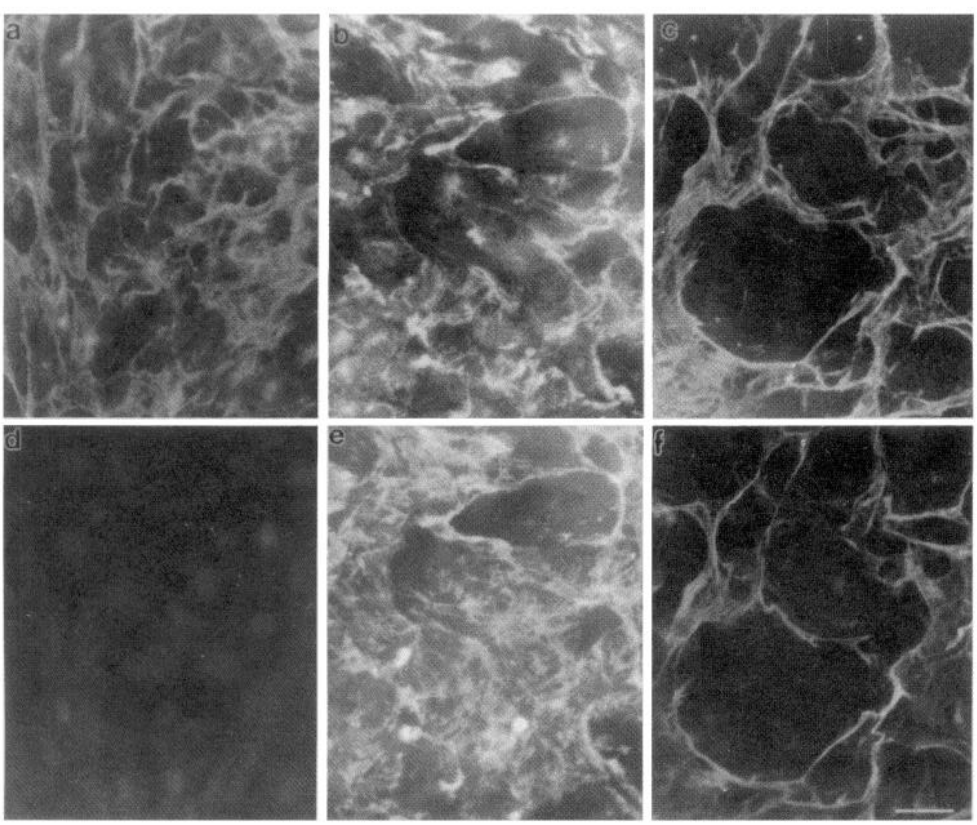

Fig. 13. Localization of exogenously added human Fn (hFn) in the matrix of CPAE monolayers co-incubated with both RGD peptides and hFn. RITC fluorescence specific for bFn antigen (*top*) and FITC fluorescence specific for hFn antigen (*bottom*) are shown. *A-C*: RITC fluorescence of CPAE monolayers fixed and permeabilized at 0, 6, and 18 h, respectively, after treatment of cells with RGD peptides (0.5 mg/ml) + hFn (600 μg/ml). *D-F*: FITC fluorescence of the identical monolayers at 0, 6, and 18 h, respectively. Bar = 40 μm.

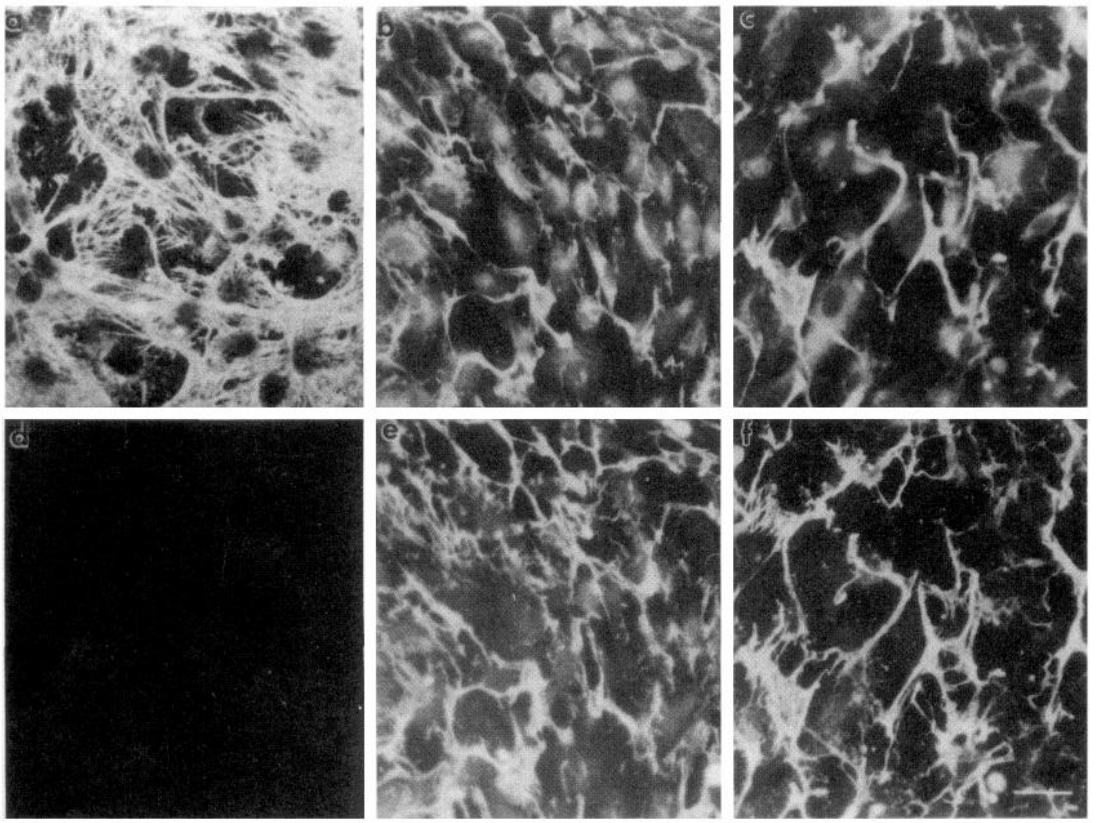

Fig. 14. Localization of exogenously added hFn in the matrix of CPAE monolayers co-incubated with both anti-$\alpha_5\beta_1$-integrins and hFn. RITC fluorescence specific for bFn antigen (*top*) and FITC fluorescence specific for hFn antigen (*bottom*) are shown. *A-C*: RITC fluorescence of CPAE monolayers fixed and permeabilized at 0, 6, and 18 h, respectively, after treatment of cells with anti-$\alpha_5\beta_1$-integrins (100 μg/ml) + hFn (600 μg/ml). *D-F*: FITC fluorescence of the identical monolayers at 0, 6, and 18 h. Bar = 40 μm.

posed to medium had 1.21 ± 0.03 μg DNA/well, while RGD peptide-treated cells had 1.07 ± 0.05 μg DNA/well ($P = 0.05$). Monolayers exposed to anti-$\alpha_5\beta_1$ did display a slight decline in DNA, i.e., 0.9 ± 0.04 μg DNA/well ($P < 0.05$) vs. the control value of 1.21 ± 0.03 μg DNA/well, but this would not explain the permeability response, since adding hFn (600 μg/ml) to the endothelial cell layer after the permeability had increased by treatment

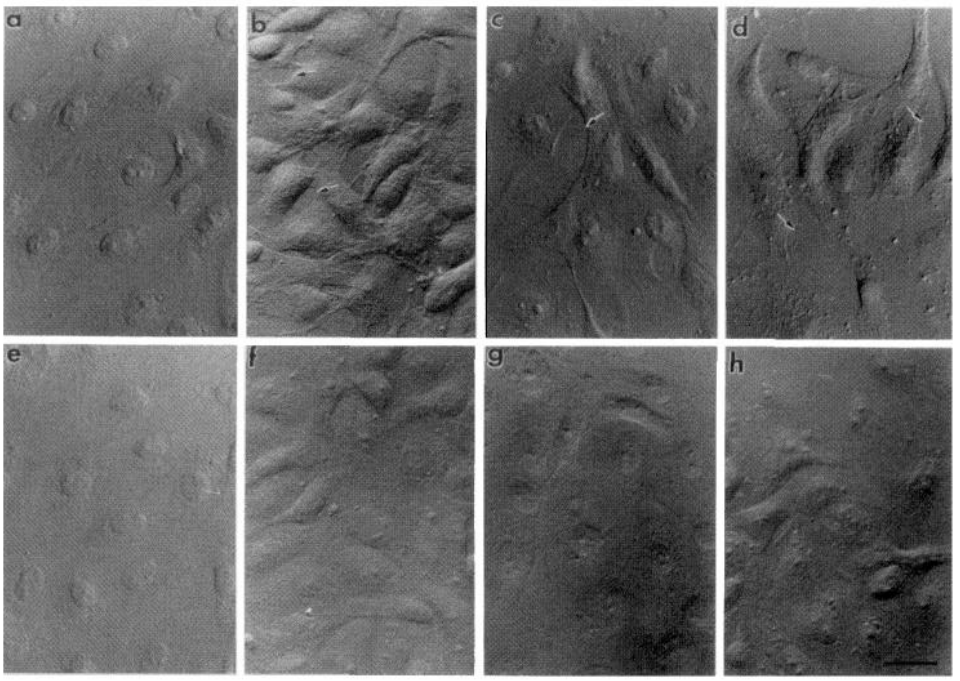

Fig. 15. Differential interference contrast (DIC) microscopy of CPAE cells treated with TNF-α, RGD peptides, and anti-$\alpha_5\beta_1$-integrins in the absence (*top*) or presence (*bottom*) of soluble hFn added to the medium. Confluent CPAE control monolayers incubated in medium for 24 h (*A* and *E*), TNF-α (200 units/ml) for 18 h (*B* and *F*), RGD peptide (0.5 mg/ml) for 18 h (*C* and *G*), and anti-$\alpha_5\beta_1$-integrins (100 μg/ml) for 24 h (*D* and *H*). *Top*: those monolayers not supplemented with hFn; *bottom*: those monolayers co-incubated with 600 μg/ml hFn. Arrows in *B*, *C*, and *D* show intracellular gaps that appear as flat oval-shaped regions between the cells. Bar = 40 μm.

with anti-$\alpha_5\beta_1$-integrins was still able to reverse permeability to normal control levels (data not shown). Thus, while cell detachment seems not to be the basis for the large permeability increase, it is very likely that the strength/magnitude of their attachment to the substrate as well as to each other was altered as confirmed by our DIC observations showing rounding up of cells and gaps between cells, a pattern reversed by incorporation of hFn.

DISCUSSION

Fibronectin, a large-molecular-weight dimeric glycoprotein, can bind to fibrin, gelatin, heparin, and collagen, and its adhesive properties can influence the attachment of cells to the ECM (26). In the lung, Fn is found in the subendothelial matrix, under epithelial cells, and in the interstitial matrix. Such localization is consistent with its speculated role in influencing endothelial as well as epithelial cell adhesion to their substrata and the integrity of the pulmonary alveolar capillary barrier (29). Septic surgical and trauma patients often display low levels of plasma Fn, which has been speculated to contribute to altered lung vascular integrity (26). Such patients also exhibit a sequestration of activated leukocytes and monocytes in their lung microvascular and interstitial compartments. The release of proteases and/or oxygen radicals from such activated inflammatory cells may elicit disruption of the subendothelial matrix and altered endothelial cell adhesion (26). In addition, cytokines, such as TNF-α, released from such activated monocytes and macrophages sequestered in the lung (32) may also contribute to acute lung vascular injury (23, 25). Indeed, purified TNF-α is capable of inducing many of the cardiopulmonary and metabolic responses seen with endotoxin infusion (32), including an increase in lung vascular permeability (23) and perhaps a loss of Fn from the ECM (24, 26, 30). This concept is supported by the rapid release of Fn containing the ED domains (ED_1-Fn) into the plasma-free perfusate after oxidant-induced vascular injury of the perfused rabbit lung (34). This isoform of fibronectin is typically found in the matrix but barely detectable in plasma. Release of ED_1-Fn from the perfused lung with vascular injury is not prevented by prior inhibition of protein synthesis (34) and may actually precede the increase in lung protein permeability (24).

Alon et al. (3) demonstrated that TNF-α binds to the NH_2-terminal domain of Fn. However, this binding is observed essentially only when Fn is immobilized on a substrate and not when Fn is in the fluid phase. Furthermore, the TNF-α-induced increase in endothelial permeability was both attenuated by co-incubation of hFn with the TNF-α as well as reversed by adding hFn after the TNF-α-induced increase in protein permeability had already taken place. Thus the direct interaction of the added soluble Fn with TNF-α cannot readily explain the protection of the endothelial barrier we observed. Moreover, reversal of protein permeability to baseline values after treatment with TNF-α did happen within 6 h after addition of medium containing soluble Fn (600 μg/ml) but not with the addition of medium alone. Interestingly, Goldblum and Sun (10) reported that when calf pulmonary artery endothelial monolayers were treated with TNF-α (200 units/ml) for 6 h and then the TNF-α-containing medium was removed, it took 22 h before such endothelial monolayers could reverse their abnormally high protein permeability back to normal. If this effect was due to TNF-α being immobilized by newly incorporated matrix Fn, a much longer time period than 6 h would be needed for permeability to normalize. Perhaps after TNF-α is removed the integrity of the endothelial monolayer can become normalized only after enough endothelial cell Fn has been synthesized, secreted, and deposited into the ECM, a process that may require 18–24 h to be completed.

Previous studies have shown that RGD-containing peptides can inhibit cell attachment as well as elicit cell detachment from either fibronectin- or vitronectin-coated surfaces (11, 21). However, RGD peptides did not inhibit the attachment of cells to collagen or laminin (11, 13). A four-amino acid-long sequence (RGDS) contained in the Fn molecule appears to be the critical sequence for this cell attachment activity (21). We observed that the addition of RGD peptides to endothelial cell monolayers did not cause any detectable endothelial cell detachment from the matrix, presumably because the cells could still remain attached to other proteins in the matrix, such as collagen and laminin. However, the RGD peptides did alter endothelial cell morphology, resulting in gaps between adjacent endothelial cells as readily observed with differential interference contrast microscopy. Excess soluble RGD peptides in the culture medium may have displaced existing interactions between RGD-dependent integrins on the cell surface and RGD attachment sites on proteins within the matrix, resulting in changing the shape of the cells, as suggested by our DIC microscopy findings.

The presence of $\alpha_4\beta_1$-integrins on the surface of human umbilical vein endothelial cells has been recently described (17); but whether these integrins exist on the surface of bovine lung endothelial cells is not known. The $\alpha_4\beta_1$-integrin is the receptor that recognizes both the CS1 and CS5 domains within the IIICS region of hFn (12, 14, 17), resulting in a non-RGD dependent interaction. The tripeptide Lev-Asp-Val (LDV) from the CS1 site in human, rat, bovine, and avian Fn can block melanoma cell spreading on a human Fn substrate, while a control Leu-Glu-Val (LEV) peptide is inactive (14). The tetrapeptide Arg-Glu-Asp-Val (REDV) derived from the CS5 site within hFn is also inhibitory for melanoma cell adhesion and spreading on hFn (17). Human umbilical vein endothelial cells will attach and spread on a REDV-grafted substrate, and this interaction can be inhibited by excess soluble REDV peptides (17); but such a site does not exist in bovine fibronectin. We initially speculated that a non-RGD site may also be playing a role in the anti-$\alpha_5\beta_1$-induced increase in permeability, since the polyclonal antibody to the human $\alpha_5\beta_1$-integrin was raised against an immunogen that contained the β_1-subunit. Thus it could bind to other β_1-containing integrins such as $\alpha_4\beta_1$. If disruption of cell

adhesion to non-RGD binding sites was the basis for the elevation of permeability, then the synthetic LDV peptide should have caused an increase in protein permeability. However, no alteration was observed with the peptide.

The protective effect relative to protein permeability we observed is very specific to Fn and apparently dependent on its incorporation into the subendothelial matrix (36, 37). Fragments of Fn, such as the 160/180-kDa fragment, which contain both RGD and non-RGD dependent cell attachment sites but lack the 27-kDa amino terminal end, which is required for matrix incorporation, cannot attenuate or reverse the TNF-α-induced increase in endothelial protein permeability (36, 37). Also, alkylation of Fn by *N*-ethylmaleimide (NEM) treatment, which limits its ability to interact with cell-associated matrix assembly sites and become assembled into the ECM (18), blocks its protective effect on the TNF-α-induced increase in endothelial protein permeability (36, 37). The specificity of the protective effect of Fn is further emphasized by the fact that two other RGD-containing human plasma proteins, i.e., vitronectin and fibrinogen, will neither incorporate into the subendothelial matrix of culture endothelial cells nor attenuate the TNF-α-induced increase in endothelial permeability (37).

We observed that the typically fine fibrillar Fn network became less uniform and the extracellular fibers in the ECM were thickened, no longer continuous, and appeared to have collapsed. This could be due to alterations in integrin function resulting in abnormal cell adhesion and/or increased release of proteases, resulting in matrix degradation. The modulation of integrin affinities and specificities has been shown to occur in many systems. For example, during terminal differentiation of human epidermal keratinocytes, the $\alpha_5\beta_1$-integrin undergoes two regulatory events: the first is a decreased ability of the integrin to bind Fn, and the second event, which happens several hours later, is an actual loss of the integrin from the cell surface (1). Phosphorylation levels of the β_1-integrin have also been correlated with changes in the affinity of integrins for both the cytoskeleton and fibronectin (31). The observations that integrin affinities are not static and can be modified supports the possibility that TNF-α may be increasing the permeability of the endothelial barrier by influencing the affinity of cell-surface RGD-dependent integrins for attachment sites in the ECM.

TNF-α treatment could also modulate surface expression of RGD-dependent integrins. For example, Defilippi et al. (7) demonstrated that treating human umbilical vein endothelial cells with TNF-α markedly downregulated the $\alpha_6\beta_1$-laminin receptor on the cell surface. This decreased expression of the $\alpha_6\beta_1$-integrin was related to a decline of α_6-mRNA in TNF-α-treated endothelial cells. However, the expression of the $\alpha_6\beta_1$-integrin was at its minimum level between 48 and 72 h after TNF-α treatment (7). In the current study, we observed a maximum change in endothelial monolayer protein permeability by 18 h after TNF-α exposure. Thus actual loss of $\alpha_6\beta_1$-integrins from the cell surface would appear not to be an explanation for the response to TNF-α observed in the present study. Treatment of human umbilical vein cells with the combination of TNF-α and IFN-γ was clearly shown to decrease surface expression of β_3-integrins, presumably due to decreased synthesis of the β_3-subunit at the translation level (8). However, as reported by Defilippi et al. (8), this modification of integrin expression was only seen when both cytokines were present, but not with either cytokine alone.

The effect of TNF-α on lung vascular integrity could be due to protease modification of the extracellular fibrillar Fn-containing network. TNF-α causes the release of both urokinase-type plasminogen activator and metalloproteases from endothelial cells (20, 33). Moreover, RGD peptides themselves as well as anti-$\alpha_5\beta_1$-integrins could potentially stimulate protease secretion from the endothelial cells. Werb et al. (35) demonstrated that adhesion of fibroblasts to immobilized Fn peptides or to immobilized antibody against the $\alpha_5\beta_1$-integrin induced both collagenase and stromelysin gene expression, whereas adhesion of fibroblasts to intact Fn did not induce this response. They suggested that intact Fn may signal the cell differently than either antibody to the $\alpha_5\beta_1$-receptor or RGD-containing peptides. Our current findings of a disruption of the endothelial barrier by TNF-α, RGD peptides, or anti-$\alpha_5\beta_1$-integrins, but attenuation of this permeability response with incorporation of intact Fn into the matrix, is consistent with this concept.

Yang et al. (38) observed that mutant murine embryos, which lacked the expression of the α_5-subunit, could still form blood vessels, but many of these vessels appeared leaky and distended. This suggests that $\alpha_5\beta_1$-integrins may function in the development and maintenance of normal vascular integrity. However, endothelial monolayer integrity could depend on both cell-cell interactions as well as cell-matrix interactions. In this regard, Lampugnani et al. (15), using both confluent human umbilical vein endothelial cell monolayers as well as freshly isolated umbilical vein endothelium, observed that the integrin heterodimer $\alpha_5\beta_1$ was located at cell-cell contact borders, but not at the free edges of cells in culture. Our current data with lung endothelial cells as well as the findings of Lampugnani et al. (15) with umbilical vein endothelial cells demonstrate that addition of either specific antibodies to $\alpha_5\beta_1$-integrins or synthetic RGD-containing peptides to confluent endothelial monolayers can alter monolayer barrier function without causing actual cell detachment (15). Endothelial barrier function also depends on the presence of intact cadherin-type junctions. Cadherins are important cell-cell adhesion molecules, and suppression of cadherin activity results in dissociation of cells in culture. Using a monoclonal antibody to an endothelial-specific cadherin called 7B4, Lampugnani et al. (16) documented that thrombin, elastase, and TNF-α/γIFn, which increase endothelial permeability, also affect the distribution of these cadherins on endothelial cell layers. Antibodies to an NH_2-cadherin-like protein on cultured

bovine endothelial cells interfered with calcium-sensitive endothelial junctions (2), providing evidence that cadherins contribute to the endothelial barrier function. Whether integrin receptors can actually stabilize cadherin-dependent adheren junctions remains to be determined.

Soluble Fn attenuated both the RGD as well as $\alpha_5\beta_1$-integrin antibody-induced increase in endothelial permeability. Incorporation of plasma Fn into the subendothelial matrix may have enhanced cell-substrate adhesion to a degree that offset the altered endothelial cell attachment induced by either the RGD peptides or $\alpha_5\beta_1$-integrin antibodies. From this perspective, perhaps the content or amount of Fn in the matrix is a major factor influencing endothelial cell spreading and thereby the barrier function of the endothelial monolayers. The hFn appeared to attenuate the increase in permeability without preventing the reorganization of the endogenous bFn in the matrix. This suggests that the ECM may indirectly modulate barrier function by influencing endothelial cell shape, cell spreading, and cell-cell adhesion. Our morphological findings of enhanced endothelial cell spreading and increased cell-cell contact after adding soluble Fn and its incorporation into matrix support this conclusion.

The cell-dependent incorporation of plasma Fn into the subendothelial matrix may provide a physiological mechanism to stabilize the endothelial barrier when the matrix is disrupted during microvascular or interstitial inflammation (5, 36). The efficiency of such a protective mechanism may be influenced by the plasma concentration of Fn, which is often very low in septic surgical, trauma, or burn patients with increased in-lung protein permeability and adult respiratory distress (26). After its intravenous infusion, soluble intact Fn will incorporate into the ECM of the lung, liver, spleen, heart, and other tissues (4, 9, 19, 26). Postoperative bacteremia in sheep will enhance the plasma disappearance of Fn and increase its incorporation into the ECM of the lung (4), perhaps reflecting a homeostatic response to maintain lung vascular integrity (26). From this perspective, a ubiquitous cell-dependent Fn matrix assembly process may maintain a balance between ongoing turnover of Fn in the ECM and the incorporation of plasma Fn into the lung subendothelial and interstitial matrices, where it may influence the lung vascular barrier.

In summary, TNF-α, RGD peptides, and $\alpha_5\beta_1$-integrin antibodies cause both a disruption of Fn in the matrix and an increase in lung endothelial protein permeability. Human plasma Fn added to the culture medium will incorporate into the subendothelial matrix and attenuate the increase in protein permeability. Our novel finding is that matrix disruption and altered endothelial permeability caused by RGD peptides or antibodies to $\alpha_5\beta_1$ as well as the protection elicited by human plasma Fn is very similar to the response seen after TNF-α. This suggests that matrix alterations resulting in impaired interaction between RGD-directed integrins and RGD sites on Fn incorporated in the matrix may be the mechanism for the TNF-induced increase in endothelial protein permeability.

The technical assistance of Corrine Giunta and Laura Mallette as well as the secretarial assistance of Debbie Moran and Maureen Davis is appreciated.

This study was supported primarily by Grant GM-21447 from the National Institute of General Medical Sciences (NIGMS). Partial support from American Heart Association Grant 92-318GS and from Grant P01-GM-40761 is also acknowledged. T. M. Curtis and S. M. Homan are predoctoral trainees in the Department of Physiology & Cell Biology, supported by the NIH-T32-HL-07194 training grant from the National Heart, Lung, and Blood Institute (NHLBI). E. Wheatley was a predoctoral trainee in the Department of Physiology & Cell Biology, supported by the NIH-T32-HL-07194 training grant from the NHLBI, and is currently a postdoctoral fellow at Stanford University School of Medicine.

Address for reprint requests: T. M. Saba, Professor and Chairman, Dept. of Physiology & Cell Biology, Box A-134, Albany Medical College, 47 New Scotland Ave., Albany, New York 12208.

Received 18 May 1994; accepted in final form 6 April 1995.

REFERENCES

1. **Adams, J. C., and F. M. Watt.** Changes in keratinocyte adhesion during terminal differentiation: reduction in fibronectin binding precedes α5β1 integrin loss from the cell surface. *Cell* 63: 425–435, 1990.
2. **Alexander, J. S., O. W. Blaschuk, and F. R. Haselton.** An N-cadherin-like protein contributes to solute barrier maintenance in cultured endothelium. *J. Cell. Physiol.* 156: 610–618, 1993.
3. **Alon, R., L. Cahalon, R. Hershkoviz, D. Elbaz, B. Reizis, D. Wallach, S. K. Akiyama, K. M. Yamada, and O. Lider.** TNF-α binds to the *N*-terminal domain of fibronectin and augments the β_1-integrin-mediated adhesion of $CD4^+$ T lymphocytes to the glycoprotein. *J. Immunol.* 152: 1304–1318, 1994.
4. **Charash, W. E., P. A. Vincent, P. J. McKeown-Longo, T. M. Saba, E. Lewis, and M. A. Lewis.** Kinetics of plasma fibronectin: increased lung tissue incorporation after postoperative bacteremia. *Am. J. Physiol.* 260 (*Regulatory Integrative Comp. Physiol.* 29): R553–R562, 1991.
5. **Cohler, L. F., T. M. Saba, E. P. Lewis, P. A. Vincent, and W. E. Charash.** Plasma fibronectin therapy and lung protein clearance with bacteremia after surgery. *J. Appl. Physiol.* 63: 623–633, 1987.
6. **Cooper, J. A., P. J. Del Vecchio, F. L. Minnear, K. E. Burhop, W. M. Selig, J. G. N. Garcia, and A. B. Malik.** Measurement of albumin permeability across endothelial monolayers in vitro. *J. Appl. Physiol.* 62: 1076–1083, 1987.
7. **Defilippi, P., L. Silengo, and G. Tarone.** α6·β1 Integrin (Laminin receptor) is down-regulated by tumor necrosis factor α and interleukin-1 β in human endothelial cells. *J. Biol. Chem.* 267: 18303–18307, 1992.
8. **Defilippi, P., G. Truffa, G. Stefanuto, F. Altruda, L. Silengo, and G. Tarone.** Tumor necrosis factor α and interferon modulate the expression of the vitronectin receptor (integrin β3) in human endothelial cells. *J. Biol. Chem.* 266: 7638–7645, 1991.
9. **Deno, D. C., T. M. Saba, and E. P. Lewis.** Kinetics of endogenously labeled plasma fibronectin: incorporation into tissues. *Am. J. Physiol.* 245 (*Regulatory Integrative Comp. Physiol.* 14): R564–R575, 1983.
10. **Goldblum, S. E., and W. L. Sun.** Tumor necrosis factor-α augments pulmonary arterial transendothelial albumin flux in vitro. *Am. J. Physiol.* 258 (*Lung Cell. Mol. Physiol.* 2): L57–L67, 1990.
11. **Hayman, E. G., M. D. Pierschbacher, and E. Ruoslahti.** Detachment of cells from culture substrate by soluble fibronectin peptides. *J. Cell Biol.* 100: 1948–1954, 1985.
12. **Humphries, M. J., A. Komoriya, S. K. Akiyama, K. Olden, and K. M. Yamada.** Identification of two distinct regions of the type III connecting segment of human plasma fibronectin that promote cell type-specific adhesion. *J. Biol. Chem.* 262: 6886–6892, 1987.

13. **Ill, C. R., E. Engvall, and E. Ruoslahti.** Adhesion of platelets to laminin in the absence of activation. *J. Cell Biol.* 99: 2140–2145, 1984.
14. **Komoriya, A., L. J. Green, M. Mervic, S. S. Yamada, K. M. Yamada, and M. J. Humphries.** The minimal essential sequence for a major cell type-specific adhesion site (CS-1) within the alternatively spliced type III connecting segment domain of fibronectin is leucine-aspartic acid-valine. *J. Biol. Chem.* 266: 15075–15079, 1991.
15. **Lampugnani, M. G., M. Resnati, E. Dejana, and P. C. Marchisio.** The role of integrins in the maintenance of endothelial monolayer integrity. *J. Cell Biol.* 112: 479–490, 1991.
16. **Lampugnani, M. G., M. Resnati, M. Raiteri, R. Pigott, A. Pisacane, G. Houen, L. P. Ruco, and E. Dejana.** A novel endothelial-specific membrane protein is a marker of cell-cell contacts. *J. Cell Biol.* 118: 1511–1522, 1992.
17. **Massia, S. P., and J. A. Hubbell.** Vascular endothelial cell adhesion and spreading promoted by the peptide REDV of the IIICS region of plasma fibronectin is mediated by integrin $\alpha_4\beta_1$. *J. Biol. Chem.* 267: 14019–14026, 1992.
18. **McKeown-Longo, P. J., and D. F. Mosher.** The assembly of the fibronectin matrix in cultured human fibroblast cells. In: *Fibronectin*, edited by D. F. Mosher. San Diego, CA: Academic Press, 1989, p. 163–179.
19. **Oh, E., M. Pierschbacher, and E. Ruoslahti.** Deposition of plasma fibronectin in tissues. *Proc. Natl. Acad. Sci. USA* 78: 3218–3221, 1981.
20. **Partridge, C. A., J. J. Jeffrey, and A. B. Malik.** A 96-kDa gelatinase induced by TNF-α contributes to increased microvascular endothelial permeability. *Am. J. Physiol.* 265 (*Lung Cell. Mol. Physiol.* 9): L438–L447, 1993.
21. **Pierschbacher, M. D., and E. Ruoslahti.** Cell attachment activity of fibronectin can be duplicated by small synthetic fragments of the molecule. *Nature Lond.* 309: 30–33, 1984.
22. **Rago, R., J. Mitchen, and G. Wilding.** DNA fluorometric assay in 96-well tissue culture plates using Hoechst 33258 after cell lysis by freezing in distilled water. *Anal. Biochem.* 191: 31–34, 1990.
23. **Redl, H., G. Schlag, and H. Lamche.** TNF- and LPS-induced changes of lung vascular permeability: studies in unanesthetised sheep. *Circ. Shock* 31: 183–192, 1990.
24. **Rizk, T., R. Rebres, P. Vincent, E. Lewis, P. J. McKeown-Longo, and T. M. Saba.** ED1-containing cellular fibronectin release into lung lymph during vascular injury with post-operative bacteremia. *Am. J. Physiol.* 264 (*Lung Cell. Mol. Physiol.* 8): L66–L73, 1993.
25. **Royall, J. A., R. L. Berkow, J. S. Beckman, M. K. Cunningham, S. Matalon, and B. A. Freeman.** Tumor necrosis factor and interleukin 1 increase vascular endothelial permeability. *Am. J. Physiol.* 257 (*Lung Cell. Mol. Physiol.* 1): L399–L410, 1989.
26. **Saba, T. M.** Fibronectin: role in phagocytic host defense and lung vascular integrity. In: *Fibronectin in Health and Disease*, edited by S. Carsons. Boca Raton, FL: CRC Press, 1989, p. 49–68.
27. **Saba, T. M., F. A. Blumenstock, D. M. Shah, R. H. Landaburu, M. E. Hrinda, D. C. Deno, J. M. Holman, Jr., E. Cho, C. Phelan, and P. M. Cardarelli.** Reversal of opsonic deficiency in surgical, trauma, and burn patients by infusion of purified human plasma fibronectin. *Am. J. Med.* 80: 229–240, 1986.
28. **Siflinger-Birnboim, A., P. J. Del Vecchio, J. A. Cooper, F. A. Blumenstock, J. M. Shepard, and A. B. Malik.** Molecular sieving characteristics of the cultured endothelial monolayer. *J. Cell. Physiol.* 132: 111–117, 1987.
29. **Stenman, S., and A. Vaheri.** Distribution of a major connective tissue protein, fibronectin, in normal human tissues. *J. Exp. Med.* 147: 1054–1064, 1978.
30. **Stolpen, A. H., E. C. Guinan, W. Fiers, and J. S. Pober.** Recombinant tumor necrosis factor and immune interferon act singly and in combination to reorganize human vascular endothelial cell monolayers. *Am. J. Pathol.* 123: 16–24, 1986.
31. **Tapley, P., A. F. Horwitz, C. A. Buck, K. Burridge, K. Duggan, R. Hirst, and L. Rohrschneider.** Analysis of the avian fibronectin receptor (integrin) as direct substrate for $pp60^{v\text{-}src}$. *Oncogene* 4: 325–333, 1989.
32. **Tracey, K. J., Y. Fong, D. G. Hess, K. R. Manogue, A. T. Lee, G. C. Kuo, S. F. Lowry, and A. Cerami.** Anti-cachectin/TNF monoclonal antibodies prevent septic shock during lethal bacteremia. *Nature Lond.* 330: 662–664, 1987.
33. **van Hinsberg, V. W. M., E. A. van den Berg, W. Fiers, and G. Dooijewaad.** Tumor necrosis factor induces the production of urokinase-type plasminogen activation by human endothelial cells. *Blood* 75: 1991–1998, 1990.
34. **Vincent, P. A., R. A. Rebres, E. P. Lewis, V. Hurst IV, and T. M. Saba.** Release of ED_1 fibronectin from matrix of perfused lungs after vascular injury is independent of protein synthesis. *Am. J. Physiol.* 265 (*Lung Cell. Mol. Physiol.* 9): L485–L492, 1993.
35. **Werb, Z., P. M. Tremble, O. Behrendtsen, E. Crowley, and C. H. Damsky.** Signal transduction through the fibronectin receptor induces collagenase and stromelysin gene expression. *J. Cell Biol.* 109: 877–889, 1989.
36. **Wheatley, E. M., P. J. McKeown-Longo, P. A. Vincent, and T. M. Saba.** Incorporation of fibronectin into matrix decreases the TNF-induced increase in endothelial monolayer permeability. *Am. J. Physiol.* 265 (*Lung Cell. Mol. Physiol.* 9): L148–L157, 1993.
37. **Wheatley, E. M., P. A. Vincent, P. J. McKeown-Longo, and T. M. Saba.** Effect of fibronectin on permeability of normal and TNF-treated lung endothelial cell monolayers. *Am. J. Physiol.* 264 (*Regulatory Integrative Comp. Physiol.* 33): R90–R96, 1993.
38. **Yang, J. T., H. Rayburn, and R. O. Hynes.** Embryonic mesodermal defects in α_5 integrin-deficient mice. *Development* 119: 1093–1105, 1993.